Full-Wave Analysis of Various Coplanar Bends and T-Junctions with Respect to Different Types of Air-Bridges

Thomas Becks, *Member, IEEE* and Ingo Wolff, *Fellow, IEEE*

Institute for Mobile and Satellite Communication Techniques
Moerser Straße 316, D-4132 Kamp-Lintfort, FRG

Abstract — **Air-bridges are indispensable to monolithic microwave integrated circuit design in coplanar waveguide technique. Based on a extension of the spectral domain analysis method to analyze three-dimensional metallization structures, various types of air-bridges within bends and T-junctions are investigated. Generalized scattering parameters are calculated in order to compare the different bridge layouts. The accuracy of the proposed method is checked by comparing with measurements.**

Introduction

During the past few years, coplanar waveguides (CPW) in MMIC's have become widely used due to several advantages compared with a conventional microstrip design. No via holes are needed to connect active devices with the ground conductor. Low dispersion of the propagation constant and the characteristic impedance for the coplanar mode (even mode). Variation of the slot and strip width offers two degrees of freedom, once the substrate height is chosen. However, there is one major drawback in dealing with a coplanar design. The parasitic coupled slotline mode (odd mode) is excited by electrically or geometrically nonsymmetrical CPW discontinuities like bends and T-junctions. Both, the even- as well as the odd-mode, are fundamental modes of the coplanar waveguide system. Therefore air-bridges become unavoidable in order to suppress the dispersive and radiating slotline mode.

Until now only two full-wave methods concerning the individual geometry of air-bridges inside the structure under consideration have been published. In [1] a three dimensional finite difference method in the frequency domain has been used to investigate the scattering behavior of single air-bridges. Results for modified air-bridge T-junctions using an FDTD algorithm were reported by [2]. Very recently, in [3, 4] an extended spectral domain method was implemented to investigate microstrip structures, for example a rectangular spiral inductor, including bondwires and air-bridges. Electromagnetic effects due to electric currents in the horizontal and vertical direction were considered by formulating the dyadic Green's function for currents pointing in all directions. Another spectral domain approach, which is better suited to handle air-bridge structures in CPW circuits, was proposed in [5, 6]. In the latter approach, the spectral domain method and image theory are used to calculate nonshielded CPW structures including air-bridges.

In the next section of this paper, the numerical method including derivation of the integral equation, application of image theory in connection with superposition principle and the technique to extract generalized S-parameters are described briefly. Afterwards the proposed method is applied to study the behavior of three types of air-bridges in a coplanar bend structure. In order to check the accuracy of the algorithm, four coplanar T-junctions on a GaAs substrate, containing three standard respectively one modified air-bridge, have been built and measured. For the even mode scattering parameters, a very good agreement over the whole frequency range, compared to the calculated results, is obtained. Various data for the conversion from the even-mode to the odd-mode within these structures will also be given. As a result of the investigations some design ideas for CPW circuit designers are determined. Finally, problems in coplanar measurements using probe tips are discussed.

W

Theory

As usual in spectral domain theory, all planar metallizations are assumed infinitely thin conductors. Nonideal metallization can be modeled by plane impedance surfaces. Considering of the coplanar structure as an aperture in a planar conducting screen of infinite extent separating two half spaces of different electromagnetic properties splits the original problem into two simpler ones [7]. After introducing magnetic surface currents $\boldsymbol{M}_S$ to restore the electric slot fields $\boldsymbol{e}_z \times \boldsymbol{E}_S = -\boldsymbol{M}_S$, the apertures are replaced by planar metallization (Fig. 1). The magnetic currents, related as shown in Fig. 1, radiate an electromagnetic field either in the upper region (a) or the lower region (b). The remaining boundary condition to be applied is the continuity of the tangential magnetic field on the slot apertures $(x, y) \in \Omega_{slot}$.

$$\boldsymbol{e}_z \times \left[\boldsymbol{H}^{\uparrow}(x, y, z = 0) - \boldsymbol{H}^{\downarrow}(x, y, z = 0)\right] = \boldsymbol{0}. \qquad (1)$$

This procedure as simple as it is, is convenient to apply the image theory to describe vertical directed parts of air-bridges. The application of the image theory is illustrated in Fig. 2. The figure shows a cross-section of an air-bridge (type A [8]); both side conductors are connected via a bridge structure located above the center conductor. Again magnetic currents can be used to restore the tangential electric fields in the slots. The horizontal directed bridge-part is modelled by electric surface current densities $\boldsymbol{J}_S^{\uparrow}$ (Fig. 2b, upper part). Electromagnetic fields excited by the vertical directed bridge-metallization can be calculated by using image theory. First, the part in z-direction is modelled by introducing an electric surface current density $\boldsymbol{J}_{ver}^{\uparrow}(y, z) = J_{ver}^{\uparrow}\boldsymbol{e}_y + J_{ver}^{\uparrow}\boldsymbol{e}_z$. Second, image currents $\boldsymbol{J}_{ver}^{\downarrow}(y, -z) = -J_{ver}^{\uparrow}\boldsymbol{e}_y + J_{ver}^{\uparrow}\boldsymbol{e}_z$ are used to replace the ground metallization plane (Fig. 2b, lower part).

CH3277-1/93/0000-0697$01.00 © 1993 IEEE

Afterwards the resulting electromagnetic fields $\boldsymbol{H}^{\uparrow}$ and $\boldsymbol{E}^{\uparrow}$ excited by $\boldsymbol{J}^{\uparrow}_{ver}$ can be described as fields excited by surface currents embedded in a homogeneous surrounding area. The resulting field components in both areas below and above the aperture have to fulfil some boundary conditions defined with the superposition principle as

$$\boldsymbol{e}_z \times \left[\boldsymbol{H}^{\uparrow}(x,y,z=0) - \boldsymbol{H}^{\downarrow}(x,y,z=0)\right] = \boldsymbol{0} \quad (2)$$
$$\text{with: } (x,y) \in \Omega_{slot},$$

$$\boldsymbol{e}_z \times \boldsymbol{E}^{\uparrow}(x,y,z=h) = Z_S \left[\boldsymbol{e}_z \times \boldsymbol{J}^{\uparrow}_S\right] \quad (3)$$
$$\text{with: } (x,y) \in \Omega_S,$$

$$\boldsymbol{e}_x \times \boldsymbol{E}^{\uparrow}(x,y,z) = Z_S \left[\boldsymbol{e}_x \times \boldsymbol{J}^{\uparrow}_{ver}\right] \quad (4)$$
$$\text{with: } (x,y,z) \in \Omega_{ver},$$

where

$$\boldsymbol{H}^{\uparrow} = \boldsymbol{H}(\boldsymbol{M}^{\downarrow}_S, \boldsymbol{J}^{\uparrow}_S, \boldsymbol{J}^{\uparrow}_{ver}, \boldsymbol{J}^{\downarrow}_{ver}), \quad (5)$$
$$\boldsymbol{H}^{\downarrow} = \boldsymbol{H}(\boldsymbol{M}^{\downarrow}_S), \quad (6)$$
$$\boldsymbol{E}^{\uparrow} = \boldsymbol{E}(\boldsymbol{M}^{\downarrow}_S, \boldsymbol{J}^{\uparrow}_S, \boldsymbol{J}^{\uparrow}_{ver}, \boldsymbol{J}^{\downarrow}_{ver}),. \quad (7)$$

Therefore, application of image theory and superposition principle projects the originally three-dimensional metallization structure onto a set of three two-dimensional metallization structures. Each field component involved in (5)-(7) can be expressed by an integral form

$$\begin{pmatrix} \boldsymbol{E}_U \\ \boldsymbol{H}_U \end{pmatrix} = \frac{1}{4\pi^2} \iint_{-\infty}^{+\infty} \begin{pmatrix} \tilde{\boldsymbol{G}}_{E,U} \cdot \tilde{\boldsymbol{U}} \\ \tilde{\boldsymbol{G}}_{H,U} \cdot \tilde{\boldsymbol{U}} \end{pmatrix} e^{j(k_x x + k_y y)} dk_x dk_y \quad (8)$$

where $\boldsymbol{U} = \boldsymbol{M}^{\downarrow}_S, \boldsymbol{M}^{\uparrow}_S, \boldsymbol{J}^{\uparrow}_S, \boldsymbol{J}^{\uparrow}_{ver}, \boldsymbol{J}^{\downarrow}_{ver}$. The tilde is indicating the spectral domain. The $\tilde{\boldsymbol{G}}_{E,U}$ and $\tilde{\boldsymbol{G}}_{H,U}$ are the dyadic Green's functions calculated in an iterative manner for a multilayered dielectric substrate. Special care must be given to the poles of the Green's functions as well as to the integration range $k_x^2 + k_y^2 \leq k_0^2$ to consider surface wave effects and radiation correctly. Combination of (8) and (2)-(7) leads to a set of three coupled integral equations. These integral equations are solved using the method of moments where all current densities electric or either magnetic are expanded in terms of rooftop basis functions. Then Galerkin's method is applied to project the integral equations onto a system of linear equations. Feeding lines are terminated in some distance from the CPW component under consideration. Impressed source magnetic current distributions [9], precomputed from the eigenvalue problem CPW line, are introduced at the end of the feeding lines. Their purpose is twice, first to excite the structure and second to match the ends of the feeding lines.

In order to form a set of linear independent equations to get the generalized scattering parameters from, about the same number of linear independent excitations of the structure has to be done. For example for a typical CPW structure, a T-junction showing no geometrical symmetries, six different excitations have to be performed during numerical analysis. The structure is containing three ports with two existing modes per feeding line. The S-parameter extraction technique used here is fully described in [4]. After any solution of the linear system the resulting coefficients (amplitudes) of the rooftops are known and the electromagnetic fields all over the component can be calculated by application of (8). The amplitudes of the backward and forward travelling waves on each feeding line can be extracted by testing the transversal fields with the precomputed transversal fields of the line eigenvalue problem. This testing procedure has to be repeated for each excitation within a testing plane on each feeding line for each propagating mode. As a result the properties of the CPW component can be described by generalized scattering parameters in the form

$$\begin{pmatrix} \boldsymbol{b}_e \\ \boldsymbol{b}_o \end{pmatrix} = \begin{pmatrix} \boldsymbol{S}_{ee} & \boldsymbol{S}_{eo} \\ \boldsymbol{S}_{oe} & \boldsymbol{S}_{oo} \end{pmatrix} \cdot \begin{pmatrix} \boldsymbol{a}_e \\ \boldsymbol{a}_o \end{pmatrix} \quad (9)$$

where the subscript e and o indicate even and odd. Therefore for example the $\boldsymbol{S}_{oe}$-matrix describes the mode conversion from the even-mode to the odd-mode.

Results

To check the accuracy of the proposed method, four T-junctions which have been built and measured by [10] were analyzed numerically. The purpose to look for these structures was to compare the air-bridge T-junction [8] with a conventional one. Layouts for both structures are shown in Fig. 3 . Additionally this comparison was made for two kinds of CPW lines attached to the junction. First a line with inner conductor 75μm and slots of 50μm and second a much smaller line witch center conductor 15μm and slot width 10μm. Both lines were built on a 410μm GaAs substrate ($\varepsilon_r = 12.9$). Characteristic impedance for the coplanar mode of such lines is approximately 50Ω. Bridge height for all air-bridge structures is 3μm.

All measurements were performed with a Cascade probe measurement setup, so only scattering parameters for the even mode could be verified. In Fig. 4 numerical results for the reflection and the transmission coefficients for the coplanar mode are compared to those available from the measurements. Both, the conventional and the modified air-bridge T-junction, are of the $75/50\mu$m-type. As can be seen, for both structures a good agreement of measured and calculated curves is obtained. The reflection coefficients S^{ee}_{11} of both structures slightly increase up to higher frequencies. This is due to the parasitic capacitance of the bridge structures. Because of the length of the bridge in the modified T-junction, the effect can be seen much more better for these structure. Nevertheless, this behaviour of the reflection coefficient causes no problems for the circuit designer.

The mode conversion from an excitation of an even mode at port one to the outgoing odd wave at port 2 is described in Fig. 5. Here of course measurements are not available. Comparison of the results for S^{oe}_{21} of both structures clearly show a much better behavior in mode conversion for the modified T-junction. As to be expected results for the small line structures (broken-lines) are up to factor of five better then those for the wider line structures (solid-lines). The results show the modified air-bridge T-junction more promising for suppression of mode conversion. In addition, the space requirements for these type of air-bridge may be better then for standard types.

As mentioned in the introduction, problems in coplanar measurements turn up when odd-mode suppression in the device under test is not made sure. Fig. 6 shows some calculated scattering parameters for a T-junction containing no air-bridges. Result of the numerical analysis is a six by six S-matrix. Broken lines indicate two parameters taken out of this matrix. In a next step, to make a first approximation for the influence of the probe tips odd modes at all ports are short circuited by enforcing $\boldsymbol{b}_o = -\boldsymbol{I} \cdot \boldsymbol{a}_o$:

$$\boldsymbol{b}_e = (\boldsymbol{S}_{ee} - \boldsymbol{S}_{eo} \cdot (\boldsymbol{S}_{oo} + \boldsymbol{I})^{-1} \cdot \boldsymbol{S}_{oe}) \cdot \boldsymbol{a}_e. \quad (10)$$

The solid lines give an impression of the resulting changes for the even scattering parameters. If odd-mode suppression is not guaranteed one has to be very careful in the interpretation of measured results.

Further results for coplanar bends, including three different types of air-bridges, will be given in the oral presentation.

Conclusion

The proposed method is a powerful and efficient tool to calculate three-dimensional CPW structures. Even individual geometries of air-bridges inside of discontinuities can be investigated systematically with this full-wave field solver. The analysis gives a straightforward method to answer questions from circuit designers about the "best" air-bridge. Comparison with available measurements show the developed algorithm as very accurate.

References

[1] Beilenhoff, K.; Heinrich, W.; Hartnagel, H. L.: The scattering behavior of air bridges in coplanar MMIC's. In: *Proc. 21th European Microwave Conf.*, S. 1131–1135, Stuttgart, 1991.

[2] Rittweger, M.; Koster, N. H. L.; Kosslowski, S.; Bertenburg, R.; Heinen, S.; Wolff, I.: Full wave analysis of a modified coplanar air-bridge T-junction. In: *Proc. 21th European Microwave Conf.*, S. 993–998, Stuttgart, 1991.

[3] Becks, T.; Wolff, I.: Full-wave analysis of 3d metallization structures using a spectral domain technique. In: *1992 IEEE MTT-S Int. Microwave Symp. Dig.*, S. 1123–1126, Albuquerque, 1992.

[4] Becks, T.; Wolff, I.: Analysis of 3d metallization structures by a full-wave spectral domain technique. In: *IEEE Trans. Microwave Theory Tech.*, MTT-40 (1992), Nr. 12, to be published

[5] Becks, T.; Wolff, I.: Calculation of three-dimensional passive structures including bond-wires, via-holes and air-bridges using the spectral domain analysis method. In: *Proc. 21th European Microwave Conf.*, S. 571–576, Stuttgart, 1991.

[6] Becks, T.: Vollwellenanalyse von passiven, dreidimensionalen Metallisierungsstrukturen mit dem Spektralbereichsverfahren. In: *Sonderforschungsbereich 254 Höchstfrequenz- und Höchstgeschwindigkeitsschaltungen aus III-V-Halbleitern Arbeits- und Ergebnisbericht 1990, 1991, 1992*, S. 392–429, Universität - GH- Duisburg, 1992.

[7] Butler, C. M.; Umashankar, K. R.: Electromagnetic excitation of a wire through an aperture-perforated conducting screen. In: *IEEE Trans. Antennas and Propagat.*, AP-24 (1976), Nr. 4, S. 456–462

[8] Koster, N. H. L.; Kosslowski, S.; Bertenburg, R.; Heinen, S.; Wolff, I.: Investigations on air-bridges used for MMICs in CPW technique. In: *Proc. 19th European Microwave Conf.*, S. 666–671, London, 1989.

[9] Wertgen, W.; Jansen, R. H.: A 3D field-theoretical simulation tool for the CAD of mm-wave MMIC's. In: *Alta Frequenza*, LVII (1988), Nr. 5, S. 203–216

[10] Naghed, M.: Private communication.

Figures

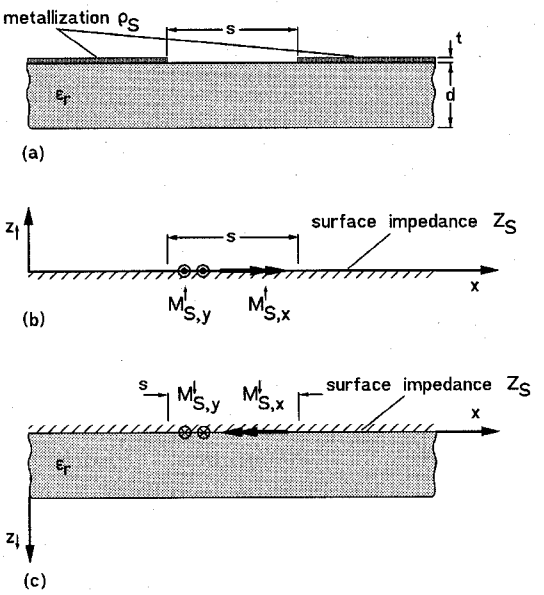

Fig 1. Step by step substitution of the original slot structure (a) by two simpler structures valid above (b) and below (c) the aperture.

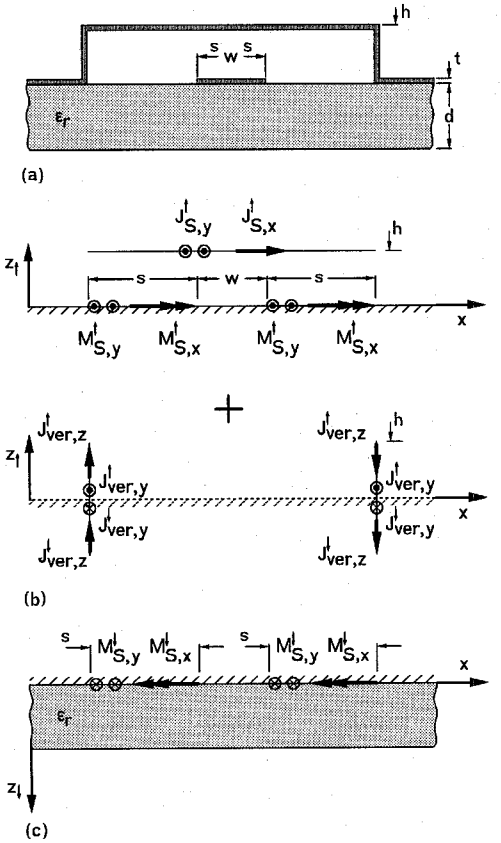

Fig 2. Reformulation of the original three-dimensional air-bridge problem (type A), cross section in (a), by projection onto a set of two-dimensional problems, valid above (b) and below (c) the aperture.

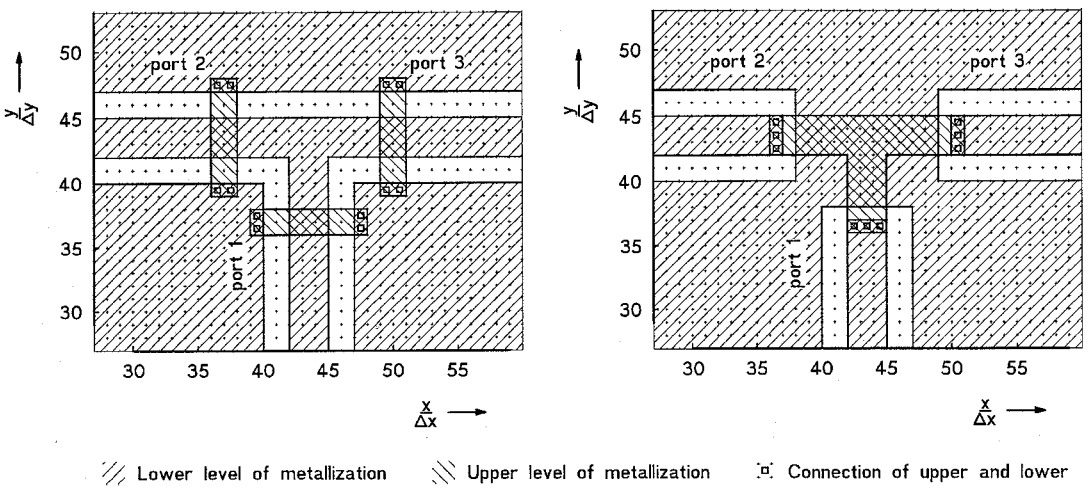

Fig 3. Layout of the conventional (left figure) and the modified (right figure) air-bridge T-junction; $\varepsilon_r = 12.9$, $d = 410\mu$m, $w = 75(15)\mu$m, $s = 50(10)\mu$m, $h = 3\mu$m.

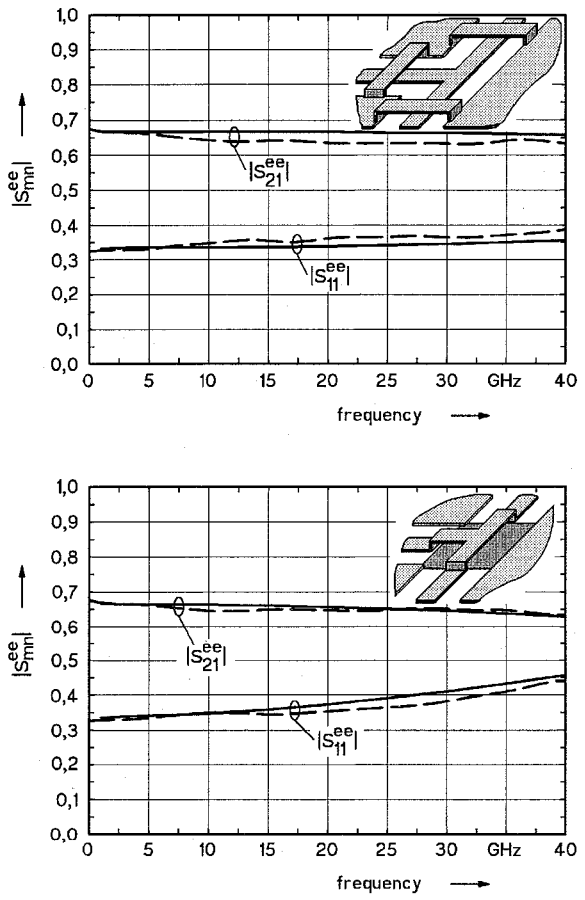

Fig 4. S-parameters of the conventional (upper figure) and the modified (lower figure) air-bridge T-junction; $w = 75\mu$m, $s = 50\mu$m. Calculated with the proposed method (—) and measured by [10] (– –).

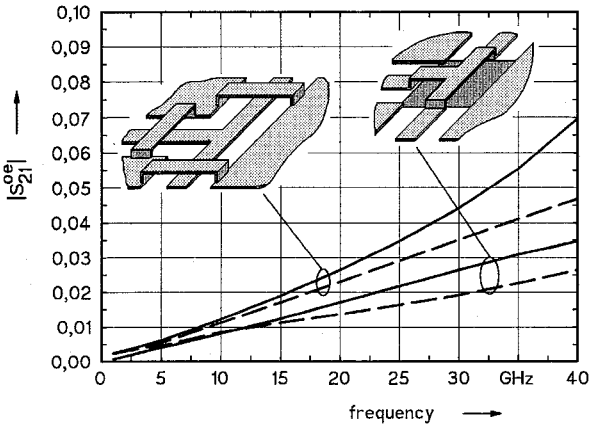

Fig 5. Mode conversion from coplanar (even) mode at port 1 to coupled slotline (odd) mode at port 2; Line geometry $w = 75\mu$m, $s = 50\mu$m (—), Line geometry $w = 15\mu$m, $s = 5\mu$m ($5 \times S_{21}^{oe}$ – –).

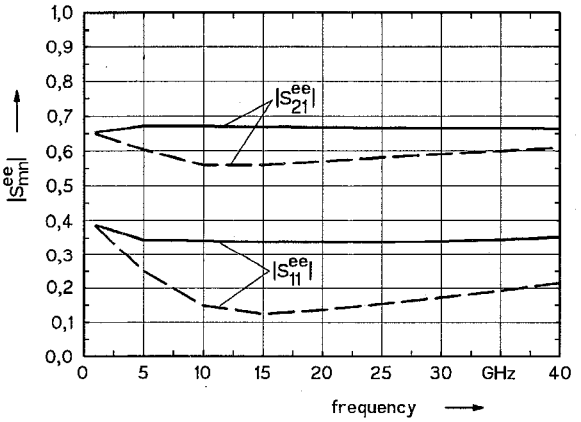

Fig 6. S-parameters of an uncompensated CPW T-junction. S_{mn}^{ee} (– –) from the generalized scattering matrix (9) and from short circuiting the odd ports by $\boldsymbol{b}_o = -\boldsymbol{I} \cdot \boldsymbol{a}_o$ in (9) (—).